ANNUAL REVIEWS

Annual Review of Fluid Mechanics

Some Recent Developments in Turbulence Closure Modeling

Paul A. Durbin

Department of Aerospace Engineering, Iowa State University, Ames, Iowa 50011;
email: durbin@iastate.edu

Annu. Rev. Fluid Mech. 2018. 50:77–103

First published as a Review in Advance on August 16, 2017

The *Annual Review of Fluid Mechanics* is online at fluid.annualreviews.org

https://doi.org/10.1146/annurev-fluid-122316-045020

Keywords

turbulent flow, laminar to turbulent transition, hybrid simulation, elliptic blending, data-driven modeling

Abstract

Turbulence closure models are central to a good deal of applied computational fluid dynamical analysis. Closure modeling endures as a productive area of research. This review covers recent developments in elliptic relaxation and elliptic blending models, unified rotation and curvature corrections, transition prediction, hybrid simulation, and data-driven methods. The focus is on closure models in which transport equations are solved for scalar variables, such as the turbulent kinetic energy, a timescale, or a measure of anisotropy. Algebraic constitutive representations are reviewed for their role in relating scalar closures to the Reynolds stress tensor. Seamless and nonzonal methods, which invoke a single closure model, are reviewed, especially detached eddy simulation (DES) and adaptive DES. Other topics surveyed include data-driven modeling and intermittency and laminar fluctuation models for transition prediction. The review concludes with an outlook.

1. INTRODUCTION

Eddy viscosity: represents averaged turbulent mixing, locally, as gradient diffusion

k: turbulent kinetic energy

ε: k's rate of dissipation

ω: 1 over the correlation timescale

Reynolds-averaged: ensemble-averaged

CFD: computational fluid dynamics

Eddy resolving: space-time resolution of chaotic fluid dynamics in a computer simulation

Turbulence closure modeling has a storied, if perhaps inelegant, history. Luminaries including G.I. Taylor, Ludwig Prandtl, A.N. Kolmogoroff, and Theodore von Kármán, among others, invoked analogies to kinetic theory and Brownian movement, as well as concepts of universality and dimensional scaling, to lay foundations of the subject. Perhaps prophetically, representing turbulent transport by an eddy viscosity underlies most of this seminal work. Today, the framework of closure modeling remains the same as that of the early pioneers: Turbulent transport is modeled by eddy viscosities, velocity covariances, and correlation timescales.

From its outset, closure modeling has been a mixture of analysis, empiricism, and analogy, directed to rather practical aims. After a period of time, during which the goal of most practical turbulence modeling was predicting bulk parameters, computer power advanced to the state that solving partial differential equations for turbulent transport became practical. Computer power led to the modern era of turbulence modeling, which is sometimes said to have begun after the 1968 Stanford conference on turbulent boundary layers. At the outset of the 1970s, researchers at Imperial College led by Brian Spalding and Brian Launder took a prominent role, with many notable contributors including Kemo Hanjalic, Wolfgang Rodi, Peter Bradshaw, Mike Gibson, Bill Jones, and Steve Pope, among others. The $k-\varepsilon$, $k-\omega$, and various Reynolds stress transport models date from this time period, albeit with precedents from earlier times and with many contributions from outside of the Imperial College circle. Algorithms for Reynolds-averaged Navier–Stokes (RANS) computation, as well as the idea of the commercial computational fluid dynamics (CFD) code, also stem from this period. Algorithms have developed systematically and progressively, and commercial CFD has grown explosively and profitably. Closure models continue to play a major role in applied CFD and remain an area of active research and development.

At times it has been suggested that RANS models would wither away and be replaced by large-eddy simulation (LES) as a consequence of rapidly increasing computer power. Certainly, greater reliance on the unaveraged Navier–Stokes equations means more accurate results. But the demise of RANS closures has not happened: The expense in computer time, man-hours, and requirements for high-resolution gridding continue to make extensive use of LES unfeasible. Laurence (2002) provided the insight that advances in computer power have enabled RANS analysis to be applied more broadly to increasingly complex configurations and that, rather than withering away, its use has expanded. This insight has been echoed by Hanjalić (2005), who noted that RANS analysis has become ingrained in engineering practice through increased reliance on user-friendly commercial CFD codes. Closure models will remain a critical element of computational fluid dynamics analysis into the foreseeable future (Slotnick et al. 2014).

Despite the persistence of RANS models in applied CFD, the niche for eddy-resolving simulation is also growing. Most relevant to the present review is the marriage of closure models and eddy-resolving simulation, termed hybrid methods (Fröhlich & Von Terzi 2008). In that vein, so-called seamless methods, which invoke the closure model throughout the whole computational domain, are within the scope of this review.

Turbulence closure modeling has been the subject of many reviews (e.g., Launder 1989, Speziale 1991, Gatski & Rumsey 2002, Hanjalić & Kenjereš 2008) and texts (e.g., Wilcox 1998, Pope 2001, Durbin & Pettersson-Reif 2010, Leschziner 2016) and is commonly reviewed in books on CFD and manuals on CFD software. The subject of turbulence closure modeling is broad, and research continues on many fronts. This review surveys a few selected areas in which closure modeling has advanced in recent years.

2. SCALAR AND TENSOR CLOSURE MODELS

When the Navier–Stokes equations are averaged, they become unclosed. In other words, there are more variables than equations. The mean flow equation contains the velocity covariance tensor, also known as the Reynolds stresses. The equations for the covariance tensor contain both higher-order correlations and nonlocality via the pressure–velocity correlation (see Pope 2001). Closure models are empirical formulas and equations that increase the number of equations to equal the number of unknowns. To meet the needs of modern CFD, closure models invoke transport equations, which provide fields of turbulence variables. Sometimes, the variables are particular to the model, having no unambiguous physical meaning; always, the aggregate model contains ambiguous features and relies heavily on empiricism.

Closure problem: upon averaging, the number of unknowns becomes greater than the number of equations

Elliptic relaxation: if L is constant, this is the modified Helmholtz equation

Isotropy: $\overline{u_i u_j} = 2/3 k \delta_{ij}$

Transport equations used in closure modeling can be grouped into those with scalar dependent variables and those with tensor variables. Examples of the former are equations for k, ε, ω, and $\tilde{\nu}$, as in the $k-\omega$, $k-\varepsilon$, or Spalart–Allmaras (S-A) models. The latter are Reynolds stress transport models, with $\overline{u_i u_j}$ or $\overline{\theta u_i}$, for example, as dependent variables. Well-established models are not reviewed here. Indeed, only two topics, elliptic blending and algebraic stress constitutive relations, are discussed.

2.1. Elliptic Blending Models

Elliptic blending and elliptic relaxation are motivated by anisotropy caused by wall proximity. As the surface is approached, the wall-normal component of intensity decreases relative to the other two. Scalar, elliptic models have two components: The first, elliptic component incorporates wall influence as a function of the turbulent length scale and of the geometry, and the second component introduces a scalar measure of anisotropy.

The second component might seem contradictory because scalars are isotropic. The measure of anisotropy is characterized as the ratio of wall-normal to total velocity variance, $\overline{v^2}/k$. This is abstracted as a scalar. It is denoted either as ζ (Hanjalić et al. 2004) or as ϕ (Laurence et al. 2004). Its isotropic value is 2/3. The eddy viscosity ν_T is defined as either $C_\mu \zeta k T$ or $C_\mu \phi k T$, where T is a correlation timescale.

The elliptic equation for f is

$$L^2 \nabla^2 f - f = -R, \qquad 1.$$

where R is a simplified pressure–strain formula in elliptic relaxation and $R = 1$ in elliptic blending. Both the $\zeta - f$ and $\phi - f$ models invoke return to isotropy and rapid pressure–strain closures for R. As an example, in the $\zeta - f$ model (Hanjalić & Kenjereš 2008),

$$R = \frac{1}{T}\left(\frac{2}{3} - \zeta\right)\left(C_1 + C_2 \frac{P}{\varepsilon}\right), \qquad 2.$$

where C_1 and C_2 are constants, T is the turbulence timescale, and P/ε is the ratio of production to dissipation of turbulent kinetic energy. L is a turbulence length scale—some combination of the integral $k^{3/2}/\varepsilon$ and the Kolmogoroff $(\nu^3/\varepsilon)^{1/4}$ scales.

The derivation of Equation 1 relates it to a two-point correlation function that appears in an exact formula for pressure–strain covariance in homogeneous turbulence (Durbin 1993, Manceau 2015). L thereby arises as a correlation length scale (Manceau et al. 2001). However, in practice, Equation 1 is used to represent nonhomogeneous wall effects.

In the $\zeta - f$ and $\phi - f$ models, Equation 1 is combined with a transport equation for the anisotropy measure, ζ or ϕ. The transport equation for either ζ or ϕ contains f as a source term.

Redistribution: transfer of amplitude between components of the Reynolds stress tensor

For example, using ζ as the dependent variable, the equation is

$$\frac{\mathrm{D}\zeta}{\mathrm{D}t} = f - \frac{P_k}{k}\zeta + \nabla\cdot\left[\left(\nu + \frac{\nu_\mathrm{T}}{\sigma_\zeta}\right)\nabla\zeta\right] + X, \qquad 3.$$

where X represents additional terms that appear in some versions of this formulation. Hence, in effect, the wall modifies the pressure–strain term via the f equation.

Billard & Laurence (2012) developed an elliptic-blending variant termed EB-$\overline{v^2}/k$. The blending function satisfies

$$L^2\nabla^2\alpha - \alpha = -1, \qquad 4.$$

with $\alpha = 0$ on walls and $\alpha \to 1$ far from the surface. In Equation 3, f is replaced by

$$(1-\alpha^3)f_\mathrm{w} + \alpha^3 f_\mathrm{h} \qquad 5.$$

to interpolate between homogeneous f_h and near-wall f_w pressure–strain formulations, with the cubic power chosen to give a correct near-wall asymptote [expressions for f_h and f_w can be found in Billard & Laurence (2012) and Lardeau & Billard (2016)]. This formulation is more numerically robust than the elliptic-relaxation version. It predicts separated flows more accurately (Billard et al. 2012).

An extension of this formulation was developed by Lardeau & Billard (2016), with extra production terms attributed to the lag between stress and strain rate, which occurs naturally in Reynolds stress transport models. Lardeau & Billard (2016) developed a scalar model of the form of Equation 3 with a contribution to the last term X that was derived from an analogy to Reynolds stress transport. Predictions of the lag elliptic blending (lag EB) $k-\varepsilon$ model improve upon the original model, as is illustrated by the example in **Figure 1**. Accurate prediction of separation and reattachment is one of the holy grails of closure modeling, and the EB-$\overline{v^2}/k$ and lag EB $k-\varepsilon$ models appear to be significant advancements toward this goal. The lag EB model has the advantage that it depends on the rate of rotation tensor Ω_{ij} so that it can be adapted to rotation and curvature by the method of Equation 17 in Section 2.3.

Elliptic blending originated as a method for tensoral closure modeling (Manceau & Hanjalić 2002, Manceau 2005). In that case, the pressure–strain (more correctly, redistribution) closure is written as

$$\phi_{ij} = (1-\alpha^2)\phi^\mathrm{w}_{ij} + \alpha^2\phi^\mathrm{h}_{ij}, \qquad 6.$$

where α solves the elliptic Equation 4. The wall term depends on a normal direction, which is defined by $\hat{\mathbf{n}} = \nabla\alpha/|\nabla\alpha|$. An explicit formula is

$$\phi^\mathrm{w}_{ij} = -\frac{5}{T}\left[\overline{u_iu_k}\hat{n}_k\hat{n}_j + \overline{u_ju_k}\hat{n}_k\hat{n}_i - \frac{1}{2}\overline{u_ku_l}\hat{n}_k\hat{n}_l(\hat{n}_i\hat{n}_j + \delta_{ij})\right]. \qquad 7.$$

The homogeneous term ϕ^h can be any redistribution model, such as the Speziale–Sarkar–Gatski formulation (Speziale et al. 1991). ϕ_{ij} appears in the Reynolds stress transport equation, written symbolically as

$$\frac{\mathrm{D}\overline{u_iu_j}}{\mathrm{D}t} = P_{ij} + \phi_{ij} - \frac{2}{3}\varepsilon\delta_{ij} + \partial_k T_{ijk}, \qquad 8.$$

where $\mathbf{P}$ is production, $\mathbf{T}$ is transport, and anisotropic dissipation is lumped into the redistribution term. The wall term is necessary to correct the wrong anisotropy built into homogeneous redistribution models. The wall term, termed pressure echo, has been recognized since the advent of Reynolds stress transport closure modeling (Durbin & Pettersson-Reif 2010). The pressure echo is a term in an elliptic, Green function solution to Poisson's equation. Manceau (2015) reviewed how that exact but unclosed term leads to elliptic blending. Billard et al. (2012) presented applications of an elliptic blending Reynolds stress model to flow separation with some impressive results,

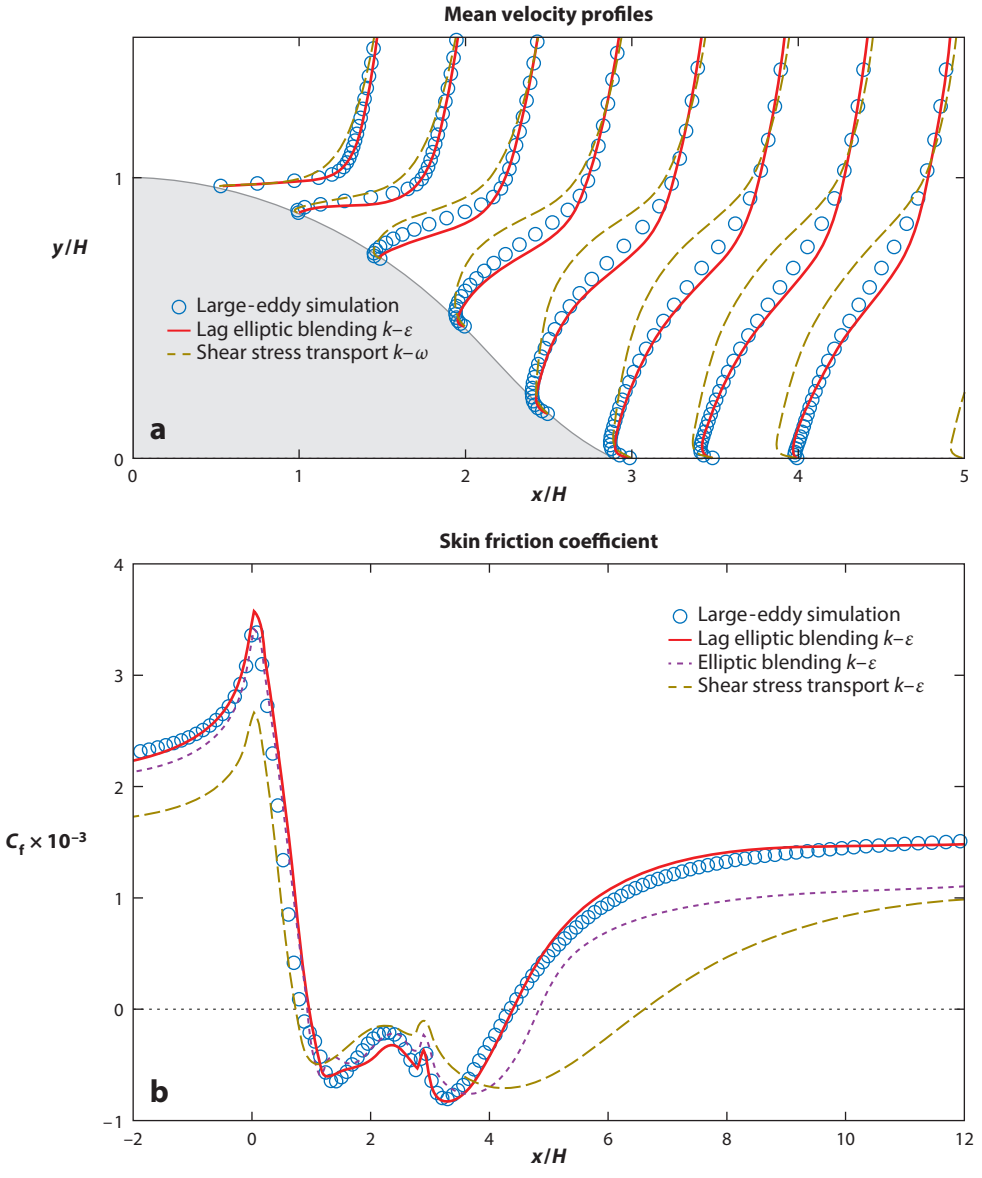

Figure 1

Flow over a curved backstep. Comparison of LES data with (*a*) mean velocity profiles and (*b*) skin friction coefficient. Figure adapted with permission from Lardeau & Billard (2016).

but also with the warning that "more physical RSM's do capture some features of the flows better than the simpler linear EVM's, although the improvements are not always consistent or uniform across different cases" (p. 146).

Elliptic relaxation and elliptic blending models have also been applied to heat transfer and to environmental flows (Kenjereš et al. 2005; Choi & Kim 2006, 2008; Hanjalić & Kenjereš 2008; Shin et al. 2008; Dehoux et al. 2011, 2017). Improved predictions are obtained for natural and mixed convective heat transfer.

2.2. Algebraic Stress Constitutive Models

Constitutive formula: formula that equates stress to a function of velocity gradient

A scalar closure must nevertheless result in a representation for the Reynolds stress second-order tensor. The connection is provided by a constitutive formula. The simplest formula is the linear, stress–strain rate, eddy viscosity relation.

The notion of eddy viscosity dates to Boussinesq in the nineteenth century. A systematic development of algebraic constitutive relations from Reynolds stress transport models began in the 1970s, with Rodi's (1976) algebraic stress approximation and Pope's (1975) closed form solution to Rodi's approximation via an integrity basis expansion (see Wallin & Johansson 2000). Over the years, researchers have enlarged upon that early work. The subjects of algebraic stress models (ASMs) and explicit algebraic stress models (EASMs) are now well established (Gatski & Jongen 2000). Those topics are mentioned in the present review because of renewed interest in using algebraic constitutive models in conjunction with recent developments in scalar closure and hybrid modeling.

The general notion is that mean flow gradients provide a tensoral representation that can be used to connect scalar turbulence variables to Reynolds stresses:

$$-\overline{u_i u}_j = kF_{ij}(T\ \partial_k U_\ell) - \frac{2}{3}k\delta_{ij}. \qquad 9.$$

Here the scalar model provides the turbulent kinetic energy k and timescale T. The timescale might be $1/\omega$ or k/ε. Eddy viscosity transport models do not have a timescale equation. In that case, Spalart (2000) replaces T by $1/|\nabla U| = (\partial_k U_j \partial_k U_j)^{-1/2}$.

The functional dependence of Equation 9 becomes an algebraic stress model upon invoking representation theorems for tensor functions of tensors, $F_{ij}(\partial_k U_\ell)$. To that end, the velocity gradient is replaced by its symmetric and antisymmetric components,

$$\begin{aligned} S^*_{ij} &= {}^1\!/_2(\partial_j U_i + \partial_i U_j)T\,, \\ \Omega^*_{ij} &= {}^1\!/_2(\partial_j U_i - \partial_i U_j)T\,, \end{aligned} \qquad 10.$$

in nondimensional form. If F_{ij} is expanded in powers of $\mathbf{S}$ and $\mathbf{\Omega}$, then representation theorems show that the expansion contains 10 independent terms, with coefficients that depend on scalar invariants (Gatski & Jongen 2000, Gatski & Rumsey 2002).

In two dimensions, the general form of Equation 9 reduces to

$$-\overline{\mathbf{uu}} + \frac{2}{3}k\mathbf{I} = C_\mu k\mathbf{S}^* + C_1 k(\mathbf{S}^*\cdot\mathbf{\Omega}^* - \mathbf{\Omega}^*\cdot\mathbf{S}^*). \qquad 11.$$

The linear eddy viscosity model is $C_1 = 0$. The coefficients C_μ and C_1 are functions of the invariants $tr(\mathbf{S}^{*2})$ and $tr(\mathbf{\Omega}^{*2})$. Other dependencies, such as on the turbulent Reynolds number ν_T/ν or on the wall distance $\sqrt{k}d/\nu$, may also be introduced. For a two-dimensional (2D) mean velocity field in three dimensions, an additional term, $C_2 k[\mathbf{S}^{*2} - {}^1\!/_3 tr(\mathbf{S}^{*2})\mathbf{I}]$, is added. In parallel shear flow, the C_μ term in Equation 11 contributes a shear stress; the nonlinear terms contribute to normal stress.

As an ASM, the coefficients in Equation 11 are arbitrary functions of the invariants. They might be specified empirically by fitting data. If they are found by solving an equilibrium approximation to a Reynolds stress transport model (see the sidebar titled The Algebraic Stress Approximation), it becomes an EASM. Then the coefficients are determined by the Reynolds stress closure.

Although an explicit solution can be found for the general, quasi-linear redistribution closure (Durbin & Pettersson-Reif 2010) via integrity basis expansions, it is too highly nonlinear to be of value. In general, nonlinear constitutive models introduce numerical stiffness. Taulbee (1992) and Wallin & Johansson (2000) developed a promising truncation. By selecting particular coefficients

THE ALGEBRAIC STRESS APPROXIMATION

One way to devise a constitutive equation is to reduce a Reynolds stress closure model to a set of algebraic equations. In homogeneous turbulence, the Reynolds stress transport equation is of the form

$$\mathrm{d}_t\overline{u_iu}_j = P_{ij} + \phi_{ij} - \frac{2}{3}\varepsilon\delta_{ij},$$

where P_{ij} is the rate of production of Reynolds stress and ϕ_{ij} is the redistribution between components of the stress tensor. Redistribution incorporates anisotropy of dissipation, so only the isotropic part $\varepsilon\delta_{ij}$ appears. One half of the trace of this equation is the turbulent kinetic energy equation

$$\mathrm{d}_t k = P - \varepsilon.$$

The equilibrium stress approximation is $\mathrm{d}_t(\overline{u_iu}_j/k) = 0$. Substituting from above, this gives

$$P_{ij} + \phi_{ij} - \frac{2}{3}\varepsilon\delta_{ij} - (P-\varepsilon)\frac{\overline{u_iu}_j}{k} = 0.$$

This is a system of equations for $\overline{u_iu}_j$ as an implicit function of the mean velocity gradient $\partial_i U_j$.

in the general linear redistribution model, Taulbee (1992) obtained the equilibrium algebraic equation

$$\left(C_\mathrm{R} - 1 + \frac{P}{\varepsilon}\right)\mathbf{b} = -\frac{8}{15}\mathbf{S} + \frac{4}{9}(\mathbf{b}\cdot\mathbf{\Omega} - \mathbf{\Omega}\cdot\mathbf{b}) \qquad 12.$$

for the anisotropy tensor, $\mathbf{b} \equiv \overline{\mathbf{uu}}/k - {}^2/_3\,\mathbf{I}$, where C_R is an empirical constant. The explicit solution of Equation 12 reduces to the two terms of Equation 11 in two dimensions, and to a sum of five terms of the integrity basis in three dimensions. The five-term solution is

$$\begin{aligned} -\overline{\mathbf{uu}} + \frac{2}{3}k\mathbf{I} = {} & C_\mu k\mathbf{S}^* + C_1 k\,(\mathbf{S}^*\cdot\mathbf{\Omega}^* - \mathbf{S}^*\cdot\mathbf{\Omega}^*) + C_2 k\left[\mathbf{\Omega}^{*2} - {}^1/_3\,tr(\mathbf{\Omega}^{*2})\mathbf{I}\right] \\ & + C_3 k\left[\mathbf{S}^*\cdot\mathbf{\Omega}^{*2} + \mathbf{\Omega}^{*2}\cdot\mathbf{S}^* - {}^2/_3\,tr(\mathbf{\Omega}^{*2}\cdot\mathbf{S}^*)\mathbf{I}\right] \\ & + C_4 k\left(\mathbf{\Omega}^*\cdot\mathbf{S}^*\cdot\mathbf{\Omega}^{*2} - \mathbf{\Omega}^{*2}\cdot\mathbf{S}^*\cdot\mathbf{\Omega}^*\right). \end{aligned} \qquad 13.$$

This is an exact solution to the system of algebraic equations represented in Equation 12, obtained as an equilibrium approximation to a Reynolds stress model—i.e., it is an EASM. The functional forms of the coefficients are given in Wallin & Johansson (2000) and in Franke et al. (2005). They invoke the consistency condition that production equals the double inner product of stress given by Equation 14 and rate of strain, $P = -\overline{\mathbf{uu}} : \mathbf{S}$. This precludes the singularity that occurred in Gatski & Speziale (1993) because production was not evaluated consistently.

There is an intuitive sense in which a five-term approximation is plausible. Because the trace of Equation 9 is an identity, it requires five components of $\overline{u_iu}_j$ to be determined by the constitutive relation. That argues for at least a five-component basis. Were $\overline{u_iu}_j$ known, one could solve for the five coefficients of the expansion (Gatski & Jongen 2000). When used as a model, the coefficients are given by formulas and $\overline{u_iu}_j$ is predicted. The reason that the general integrity basis has more than five components is that elements of any five-component basis can vanish for certain

ROTATING TURBULENT SHEAR FLOW

Rotation reduces turbulent intensity when the shear is in the direction of rotation and increases it where they are opposite. In plane Poiseuille channel flow, if the flow is left to right, convection will rotate a small material line near the lower (upper) wall in the clockwise (counterclockwise) direction. If the channel is rotated clockwise, turbulent intensity decreases near the lower wall and increases near the upper. The mean velocity profile becomes asymmetric, unlike rotating laminar channel flow.

combinations of rate of rotation and rate of strain. So the ten-component basis provides complete generality.

The full formulation of Wallin & Johansson (2000) adds blending functions (not elliptic) to adapt it to near-wall behavior. Franke et al. (2005) tested it in aerodynamic flows, using the $k-\omega$ model for the scalar terms. They found that the nonlinear constitutive model provided some improvement over the linear eddy viscosity model. Weinmann & Sandberg (2009) also found that either a 2D or 3D nonlinear constitutive relation provided improvement in a wing–body junction flow, while providing no benefit in separated flow over an axisymmetric hump.

Rumsey et al. (2000) made a suggestion that might improve the accuracy of algebraic stress models in curved flow. If the algebraic stress approximation is applied in a rotating frame, Coriolis acceleration ($\mathbf{b}\cdot\boldsymbol{\Omega}^{\mathrm{F}}-\boldsymbol{\Omega}^{\mathrm{F}}\cdot\mathbf{b}$) is added to the left side of Equation 12. Rumsey et al. (2000) found that replacing frame rotation by streamline curvature, by the method of Equation 17 in the next section, improved predictions of curved channel flow.

2.3. Rotation, Curvature, and Buoyancy

By their nature, scalar models do not respond appropriately to directional forces, such as those due to system rotation, streamline curvature, or buoyancy. These affect individual components of the Reynolds stress tensor. For instance, rotation can suppress or enhance turbulence, as a consequence of centrifugal acceleration in the radial direction, outward from the center of curvature (see the sidebar titled Rotating Turbulent Shear Flow). A scalar formula does not distinguish directional components of Reynolds stress, so the correct phenomenology is inherently absent.

2.3.1. Unification of rotation and curvature. However, models based on transport equations for scalar variables are workhorses of applied CFD. In the interest of improving their robustness, patches have been devised to sensitize such models to curvature and rotation. Early ideas (reviewed in Durbin 2011) were formulated for nearly parallel flows. Recent interest has been in formulations for general flows. Proposals have been made to base them on streamline curvature, but streamlines are not Galilean invariant. For that reason, efforts to literally represent streamline curvature have been supplanted by a method that unifies rotation and curvature via the rate of rotation of the principal axes of the rate-of-strain tensor (Spalart & Shur 1997, Wallin & Johansson 2002).

The rate-of-strain tensor is symmetric, so it can be expressed as

$$\mathbf{S}=\sum_{\alpha=1}^{3}\lambda_\alpha\mathbf{e}^\alpha\mathbf{e}^\alpha, \qquad 14.$$

where the $\mathbf{e}$'s are unit eigenvectors and the λ's are eigenvalues. Unit vectors can only change by rotating: $\mathrm{d}_t\mathbf{e}^\alpha=\Omega^{\mathrm{S}}_{\alpha\beta}\cdot\mathbf{e}^\beta$. The rotation rate tensor $\Omega^{\mathrm{S}}_{\alpha\beta}$ can be computed from the mean velocity

field. It has been used to parameterize effects of streamline curvature and system rotation, as explained below.

To begin, I provide some remarks on computing $\Omega^{\mathrm{S}}_{\alpha\beta}$. On the grounds of computational efficiency, Spalart & Shur (1997) introduced the Spalart–Shur tensor:

$$\mathbf{W}^{\mathrm{SS}} \equiv \frac{\mathbf{S}\cdot D_t\mathbf{S} - D_t\mathbf{S}\cdot\mathbf{S}}{2|\mathbf{S}|^2}. \qquad 15.$$

In two dimensions, Equation 15 equals the exact rotation tensor. Wallin & Johansson (2002) derived the connection of the Spalart–Shur tensor to rotation of the principal axes in three dimensions. If rotation vectors are introduced via $w_i^{\mathrm{SS}} \equiv \frac{1}{2}\varepsilon_{ijk}W_{jk}^{\mathrm{SS}}$ for the Spalart–Shur tensor and $\Omega_{ij}^{\mathrm{S}} = \varepsilon_{ijk}\omega_k^{\mathrm{S}}$ for the rotation of eigenvectors, then the exact relation between the Spalart–Shur tensor and the rotation rate of the principal axes is

$$w_i^{\mathrm{SS}} = \omega_i^{\mathrm{S}} - \frac{3\mathbf{S}_{ij}^2}{2|\mathbf{S}|^2}\omega_j^{\mathrm{S}}. \qquad 16.$$

Given $\mathbf{w}^{\mathrm{SS}}$, the matrix on the right of Equation 16 can be inverted via the Cayley–Hamilton theorem (Wallin & Johansson 2002), or Equation 16 can be solved as a set of three simultaneous equations for ω_i^{S}. In two dimensions, $\boldsymbol{\omega}^{\mathrm{S}}$ is in the x_3 direction, so that $\boldsymbol{\Omega}^{\mathrm{S}} = \mathbf{W}^{\mathrm{SS}}$.

This surrogate for curvature and rotation, then, is introduced into models. It represents a unification of rotation and curvature because, in a rotating coordinate system, $\boldsymbol{\Omega}^{\mathrm{S}}$ includes the system rotation tensor. A model that was devised for system rotation is made into a model for both rotation and streamline curvature by replacing coordinate frame rotation $\boldsymbol{\Omega}^{\mathrm{F}}$ by rotation of the rate of strain $\boldsymbol{\Omega}^{\mathrm{S}}$; that is, just substitute $\boldsymbol{\Omega}^{\mathrm{F}} \rightarrow \boldsymbol{\Omega}^{\mathrm{S}}$.

For instance, the absolute rotation tensor is

$$\boldsymbol{\Omega}^{\mathrm{A}} = \boldsymbol{\Omega} + \boldsymbol{\Omega}^{\mathrm{F}},$$

where $\boldsymbol{\Omega}$ is the vorticity tensor relative to a rotating frame. $\boldsymbol{\Omega}^{\mathrm{A}}$ appears in some models. One simply redefines $\boldsymbol{\Omega}^{\mathrm{A}}$ as

$$\boldsymbol{\Omega}^{\mathrm{A}} = \boldsymbol{\Omega} + \boldsymbol{\Omega}^{\mathrm{S}}. \qquad 17.$$

In Reynolds stress models, frame rotation enters via

$$\boldsymbol{\Omega}^{*} = \boldsymbol{\Omega} + C_{\mathrm{r}}\boldsymbol{\Omega}^{\mathrm{F}},$$

where C_{r} is a model constant (Speziale et al. 1991, Wallin & Johansson 2002). The analogy between curvature and rotation is invoked by replacing $\boldsymbol{\Omega}^{\mathrm{F}}$ with $\boldsymbol{\Omega}^{\mathrm{S}}$ to obtain

$$\boldsymbol{\Omega}^{*} = \boldsymbol{\Omega} + C_{\mathrm{r}}\boldsymbol{\Omega}^{\mathrm{S}}. \qquad 18.$$

Hellsten (1998) sensitized the $k-\omega$ model to coordinate system rotation via a function of the Bradshaw number [he simply replaced a constant value of $C_{\omega_2} = 3/40$ by $3/40(1 + 3.6Br)$]. An equilibrium solution in rotating homogeneous shear flow shows this to stabilize turbulence for rotation numbers above 0.24 or below −1.24 (Durbin 2011), which are approximately in agreement with experiments. Khodak & Hirsch (1996) proposed the invariant definition

$$Br = \frac{|\boldsymbol{\Omega}^{\mathrm{A}}|(|\boldsymbol{\Omega}^{\mathrm{A}}| - |\mathbf{S}|)}{|\mathbf{S}|^2}$$

of the Bradshaw number. The replacement, stated in Equation 17, makes this a curvature Bradshaw number. Arolla & Durbin (2013) applied the method of Equation 17 to other models that incorporate system rotation via invariants of the velocity gradient. It was validated by computations of rotating, curved, and swirling flows.

Shur et al. (2000) devised a function of the parameter

$$\tilde{r} = \frac{|\mathbf{S}|^2 \boldsymbol{\Omega} : \mathbf{W}^{SS}}{(|\mathbf{S}|^2 + |\boldsymbol{\Omega}|^2)^2}$$

to enhance or suppress production of eddy viscosity, depending on whether curvature was stabilizing or destabilizing. It was validated in rotating and curved channels.

2.3.2. Buoyancy. Methods for incorporating buoyancy in stratified shear flow are well established. Stability functions are introduced to parameterize mixing as a function of the Richardson number. The stability functions can be derived from second moment closure. Early analyses used overly simple pressure–strain models (Mellor & Yamada 1982). Canuto et al. (2001) developed an updated version. Equilibrium analysis of stratified shear flow shows how the stability functions, or simply the equilibrium curve of Sk/ε, suppress turbulent energy above a critical Richardson number (Canuto et al. 2001, Ji & Durbin 2004). The critical Richardson number is not entirely certain—values range from 0.25 to 1.0.

The effects of buoyancy have been especially hard to capture in the problem of flow along a vertical, heated wall. Let θ stand for temperature. The usual scalar diffusion hypothesis, $-\overline{\mathbf{u}\theta} = \alpha_T \nabla\Theta$, gives quite poor results. More generally, one can propose a tensoral relation $-\overline{\mathbf{u}\theta} = \alpha_T \cdot \nabla\Theta$. The generalized gradient diffusion hypothesis asserts that α_T is proportional to $\overline{\mathbf{uu}}$ (Suga & Abe 2000). However, this is incorrect: $\overline{\mathbf{uu}}$ is a symmetric matrix and the diffusion matrix is decidedly not symmetric. That is known from experiment and direct numerical simulation (DNS), and also can be deduced from the transport equation for $\overline{\mathbf{u}\theta}$. Kenjereš et al. (2005) proposed an algebraic closure of that transport equation in the form

$$\left(\mathbf{I} - c_1\mathbf{b} + c_2 T\,\nabla\mathbf{U}\right) \cdot \overline{\mathbf{u}\theta} = -c_3 T\,\left(\overline{\mathbf{uu}} \cdot \nabla\Theta + c_4 \beta \mathbf{g}\overline{\theta^2}\right), \qquad 19.$$

where $\mathbf{b}$ is the Reynolds stress anisotropy tensor and T is the turbulence timescale. This differs from previous models by adding the anisotropic relaxation term $c_1\mathbf{b}$. If the matrix on the left is inverted, the first term on the right becomes a diffusion tensor. The velocity gradient on the left makes the diffusion tensor asymmetric. The second term on the right provides a buoyant contribution to heat flux. Kenjereš et al. (2005) showed how this formulation captures buoyancy more accurately. Suga & Abe (2000) simply posed an asymmetric α_T, with asymmetry introduced by the vorticity tensor. They also included an anisotropy term and showed that it improves agreement to data. A more extensive discussion of scalar flux closure options can be found in Hanjalić & Launder (2011).

3. ADDING TRANSITION

The computational domain often includes a laminar to turbulent transition. That may have either a primary or a secondary effect on the turbulent flow prediction. Whether or not a transition occurs may determine whether the boundary layer is separated or attached. Or, the length of the surface in which the boundary layer is laminar might be needed for overall drag prediction.

The laminar to turbulent transition is classified into bypass and orderly modes (Zaki 2013). Bypass dominates when an attached boundary layer is subjected to free-stream disturbances, such as ambient turbulence or incident wakes. It is mediated by streaks in the laminar boundary layer. Orderly transition is mediated by instability waves. It is seen under very quiet streams, in strong adverse pressure gradients, in boundary layers with cross-flow, or in supersonic flows. Instability waves also dominate in separated flow and transition often occurs rapidly after separation. In some

BOUNDARY LAYER TRANSITION

The laminar to turbulent transition in boundary layers can be envisioned as a rise in the average level of skin friction, occurring at some downstream distance. Then the basic objective of a model is to predict where that rise occurs. The levels before and after the rise are given by the laminar and turbulent values.

cases, both streaks and instability waves arise and interact to cause mixed-mode transition (Liu et al. 2008).

Transition in boundary layers has traditionally been accommodated by data correlations. The correlation specifies a transition point, usually stated as the momentum thickness Reynolds number at transition (see the sidebar titled Boundary Layer Transition). The solution is laminar up to transition; the turbulence model is invoked post-transition. Modern, applied CFD requires a more flexible approach.

Adding the transition to Reynolds-averaged closures has presented a great challenge to modelers. Three approaches have been devised: (*a*) rely on the closure model to transition from a laminar to a turbulent solution, (*b*) use a data correlation to decide when to switch from laminar to turbulent flow, or (*c*) devise additional transport equations to represent the transition. In this last category, two approaches have been pursued. The first invokes an equation for an intermittency function $\gamma(\mathbf{x}, t)$, which is 0 in laminar flow and 1 in turbulent flow. The second is to develop a separate equation for the kinetic energy of velocity fluctuations k_L in the laminar region upstream of transition and to model how it is transferred into turbulent kinetic energy.

The oldest approach is to switch from a laminar to a turbulent computation at a prescribed transition point. Abu-Ghannam & Shaw (1980) proposed a correlation for bypass transition that becomes

$$R_{\Theta\,\mathrm{tr}} = 163 + e^{6.91 - Tu} \qquad 20.$$

under zero pressure gradient. Tu is the turbulence intensity as a percentage, $100\sqrt{\overline{u^2}}/U$, measured in the free stream. The transition is specified to occur where the local momentum thickness Reynolds number exceeds this critical value. The full correlation accounts for pressure gradients as well. Suzen & Huang (1999), among others, have proposed variants of the Abu-Ghannam & Shaw correlation. However, it can be difficult, if not impossible, to compute momentum thickness in a complex flow.

3.1. Reliance on the Turbulence Model

It is not uncommon to encounter regions of purely laminar flow or buffeted laminar flow in applications. For instance, turbine blades often operate at low enough Reynolds numbers to encounter significant portions of laminar flow on their surface, but the blades are subjected to external turbulence, so their boundary layers are better described as buffeted laminar layers (Hodson & Howell 2005). In such instances, there are irregular fluctuations in the laminar region, and the rest of the flow is turbulent. The overall flow calculation must be done with a turbulence model. Perhaps one can dispense with a transition model and rely on the turbulence closure to return a nearly laminar solution in the buffeted region and to predict transition. Is this a plausible approach?

Intermittency: the fraction $0 \leq \gamma \leq 1$ of the time that the flow is turbulent

On the face of it, the answer is no. Closures are developed for fully turbulent conditions and calibrated with turbulence data. However, most transport equation models do converge to a laminar

solution at low Reynolds number and to a turbulent solution at sufficiently high Reynolds number; in this sense, the model equations evidence a transition between laminar and turbulent solution branches. So relying on the closure model may not be entirely irrelevant, but neither is it entirely justified. Savill (1999) and Westin & Henkes (1997) explored whether low–Reynolds number $k-\varepsilon$ models can imitate bypass transitions. In some cases they found satisfactory transitional behavior. Pecnik et al. (2005) found satisfactory boundary layer transitions in calculating a turbine stage using the v^2-f model, as did Wu & Durbin (2000) for wake-induced transitions. Wilcox (1994) suggested that low–Reynolds number modifications could enable $k-\omega$ to be used in transitional flow. (It should be remarked that the term low Reynolds number refers to the near-wall region of fully turbulent flow.)

However, the switch from laminar to turbulent solutions in the standard forms of the $k-\omega$ model, $k-\omega$ shear stress transport (SST) model, and S-A model occurs at a far too low Reynolds number. Despite some successes, the turbulence model is not, in fact, a method to rely on. When accurate predictions of the laminar and transitional regions are needed, the turbulence model must be supplemented explicitly by a method to predict transition.

3.2. Intermittency Equation

After the transition criterion $R_\Theta > R_{\Theta\,\mathrm{tr}}$ (e.g., Equation 20) is met, Dhawan & Narasimha (1958) proposed that turbulent energy could be ramped up by an intermittency function, which increases across the transition region from the laminar value of 0 to the turbulent value of 1. They suggested a half-Gaussian shape: $\gamma = 1-\exp[-(x-x_{\mathrm{tr}})^2/\ell_{\mathrm{tr}}^2]$, where $x > x_{\mathrm{tr}}$. Lodefier et al. (2004) derived the form of an intermittency transport equation from that Gaussian shape:

$$\mathrm{D}_t\gamma = 2(\gamma-1)\sqrt{\gamma}\,\frac{|\mathbf{u}|}{\ell_{\mathrm{tr}}} + \nabla\cdot[(\nu+\nu_{\mathrm{T}})\nabla\gamma], \qquad 21.$$

where ℓ_{tr} is a transition length. This is a base for more elaborate formulations, which include a sink term as well a source:

$$\frac{\mathrm{D}\gamma}{\mathrm{D}t} = P_\gamma - E_\gamma + \nabla\left[\left(\frac{\nu}{\sigma_l}+\frac{\nu_{\mathrm{T}}}{\sigma_\gamma}\right)\nabla\gamma\right]. \qquad 22.$$

Langtry & Menter (2005) and Menter et al. (2006) included a second equation in their $\gamma-R_{\mathrm{T}}$ model. The R_{T} equation diffuses a data correlation from the free stream into the boundary layer. Then the model predicts both transition onset and intermittency in the transition region. Langtry & Menter (2005) rewrote the source minus the sink term on the right side of Equation 22 as

$$2|\mathbf{S}|(\gamma-1)\sqrt{\gamma f_{\mathrm{onset}}}\,f_{\mathrm{length}} + (0.06-50.0\gamma)F_{\mathrm{turb}}|\Omega|\gamma,$$

where f_{onset} and F_{turb} are complicated, highly empirical functions. The model was published without the formula for f_{length}, which was proprietary. Suluksna et al. (2009) developed the missing information and published a full statement of this model.

An additional objective was to make the transition depend on local variables, rather than the integral boundary layer thickness Θ, as in Equation 20. To that end, the local parameter

$$R_v = \frac{|S|d^2}{2.193\nu},$$

where d is distance from the wall, is used in place of R_Θ.

The intermittency method is predicated on the underlying RANS model predicting early transition. Then transition is suppressed by multiplying either production or the eddy viscosity by $\gamma(\mathbf{x}) \le 1$. As γ rises from zero to one, the model is switched on.

A question arose as to whether transition can be predicted by a single intermittency equation. Durbin (2012) and Ge et al. (2014) developed an intermittency equation that predicts the transition with neither an adjoined R_T equation nor a data correlation per se. In this approach, transition is controlled by both a source/sink and a diffusion of free-stream turbulence into the boundary layer. The source/sink is written

$$F_\gamma |\Omega| \, (\gamma_{\max} - \gamma) \sqrt{\gamma} - G_\gamma F_{\mathrm{turb}} |\Omega| \gamma^{1.5},$$

where F_γ, G_γ, and F_{turb} are complicated functions of the nondimensional, Galilean-invariant parameters

$$R_\mathrm{t} \equiv \frac{\nu_\mathrm{T}}{\nu}, \; T_\omega \equiv R_\mathrm{t} \frac{|\Omega|}{\omega}, \; R_\nu \equiv \frac{d^2 |\Omega|}{2.188 \nu},$$

where d is wall distance. σ_γ was set to 0.2 in Equation 22 to control diffusion into the boundary layer.

Menter et al. (2015) subsequently proposed a single γ equation, which they characterized as a reduction of the $\gamma - R_\mathrm{T}$ model. However, it invoked Galilean-invariant parameters similar to those above, rather than the Galilean-dependent parameters of their earlier model.

Although the $\gamma - R_\mathrm{T}$ model is devised to be used with the two-equation, $k - \omega$ turbulence model, Medida & Baeder (2011) devised a reduced version for use with the one-equation, S-A eddy viscosity transport model.

The model of Ge et al. (2014) was extended to roughness-induced transitions by Ge & Durbin (2015). They used a displaced origin as a function of wall roughness to modify the model. In order to represent roughness, Dassler et al. (2010) added a transport equation for roughness amplification to the model of Langtry & Menter (2005).

Wang & Fu (2011) proposed a single γ equation of the form of Equation 22, without a separate data correlation equation, for supersonic and hypersonic transition. They introduced timescales to represent orderly transitions by breakdown of Mack waves.

A disconcerting aspect of this type of model is that the sink term E_γ must establish a laminar boundary layer. The intermittency equation is solved everywhere, including the laminar boundary layer; a region of $\gamma = 0$ must be created by its sink term in order to define the laminar zone. That is unlike a simple data correlation, for which one computes a laminar boundary layer and then switches on the turbulence model.

3.3. Laminar Fluctuations

A second approach has a closer connection to the phenomenon of transition. Mayle (1991) proposed that the transition could be modeled through consideration of laminar fluctuation energy. That might at first seem a perverse notion: a laminar turbulent kinetic energy, denoted k_L. On second consideration, it is not so odd: The laminar fluctuating energy can be construed to represent instability waves or the streaks seen prior to the bypass transition (Zaki 2013). Such ideas are attractive, even though streaks and instability waves do not enter directly into these models. Moreover, streaks and instability waves are only precursors to the transition. In isolation, they are not the cause of turbulence; it is spawned when they break down through secondary processes.

The key elements of the model are the production of laminar fluctuations and the transfer of energy from laminar to turbulent fluctuations. Walters & Leylek (2004) and Walters & Cokljat (2008) proposed the form

$$\mathrm{D}_t k_\mathrm{L} = 2 \nu_{\mathrm{T}\ell} |S|^2 - R - \varepsilon_\mathrm{L} + \nabla \cdot (\nu \nabla k_\mathrm{L}), \qquad 23.$$

in which $2\nu_{T\ell}|S|^2$ is the rate of production of laminar fluctuations, ε_L is a dissipative term, and R transfers energy from laminar to turbulent fluctuations. To accommodate both bypass and orderly transitions, the laminar region eddy viscosity is the sum of two terms:

$$\nu_{T\ell} = \nu_{BP} + \nu_{ord}.$$

Hybrid: a combination of eddy-resolving simulation and a RANS closure

The term R in Equation 23 represents breakdown of laminar fluctuations into turbulence. The same term, with a positive sign, is added to the turbulent energy equation:

$$D_t k = 2\nu_T|S|^2 + R - \varepsilon + \nabla \cdot \left[\left(\nu + \frac{\nu_T}{\sigma_k}\right)\nabla k\right]. \qquad 24.$$

Walters & Leylek (2004) invoked $k - \varepsilon$ for the turbulence model and Walters & Cokljat (2008) invoked $k - \omega$.

Lopez & Walters (2016) proposed a variant of the laminar kinetic energy approach in which a velocity variance $\overline{v^2}$ is used instead of k_L. This variable was motivated by the role of wall-normal fluctuations in causing transitions. However, in fully turbulent flow it becomes the turbulent kinetic energy, $\overline{v^2} = k$. The new model is similar to that of Walters & Cokljat (2008), but fixes seriously inaccurate predictions of free-shear flows by the earlier model.

Kubacki & Dick (2016) reduced the laminar fluctuation model to a simple algebraic formula. They were able to predict transition on turbine blades.

Lardeau et al. (2004) combined a laminar fluctuation model with a nonlinear constitutive model (Section 2.2) based on $k - \varepsilon$. They represented the total fluctuating energy as $\gamma k_T + (1 - \gamma)k_L$. However, their model retains a data correlation for transition and the semi-Gaussian form of Dhawan & Narasimha (1958) for the intermittency function.

Transition prediction is safest when it is rooted in a data correlation. At the present time, the $\gamma - R_T$ model is the most successful for that reason. Laminar fluctuation models have not achieved the same level of predictive consistency.

4. USING RANS AS A HYBRID

Often RANS does not predict mixing in detached shear layers well. Eddy-resolving simulation is more accurate but more costly. Is there a compromise between the expense of eddy simulation and the efficiency of RANS modeling? Hybrid methods are motivated by this question. They enable eddy-resolving simulation on grids that are far too coarse for DNS and generally too coarse for wall-resolved LES. The grids at least have to be adequate for Reynolds-averaged computation. Fröhlich & Von Terzi (2008) extensively reviewed hybrid simulation.

When it is used as a hybrid, the RANS model becomes dominant in some parts of the flow—especially near walls—while an eddy-resolving simulation, with a subgrid model, prevails elsewhere. The terms zonal and nonzonal (Walters et al. 2013) are sometimes used. Zonal means that a region of the computational domain is prescribed in advance as the RANS zone, and the remainder is prescribed as the eddy simulation zone. Most work of this persuasion has come from the LES community, which has approached it as appending a RANS zone onto an LES (see Bose & Park 2018 in this volume).

Here we are concerned only with nonzonal methods. Most work of that persuasion has come from the RANS community, modifying the closure model to allow turbulent dynamics to occur. There are no RANS and eddy simulation zones per se.

One also can refer to seamless methods (Hanjalić & Kenjereš 2008) and automatic, seamless methods (Slotnick et al. 2014). It is unclear whether the terms nonzonal and seamless are distinct in prior usage: We will distinguish seamless methods as those which use only a single closure

model through the domain. The alternative is a combination of models that acts like RANS or LES, depending on which is dominant.

In a nonzonal method, one computes 3D, time-evolving solutions to the Navier–Stokes equation

$$\frac{\mathrm{D}\mathbf{U}}{\mathrm{D}t} = -\frac{1}{\rho}\nabla p + \nu\nabla^2\mathbf{U} - \nabla\cdot\boldsymbol{\tau} \qquad 25.$$

in the entire domain, with a model for the unclosed stress $\boldsymbol{\tau}$. Various substitutions for the unclosed stress cause the computation to emulate Reynolds-averaged or turbulence-resolving solutions. In the latter case, various substitutions cause the computation to be either an LES or a hybrid simulation.

The hybrid simulation adds dynamic equations for the closure. For example, for $k-\omega$, they are

$$\begin{aligned}\frac{\mathrm{D}k}{\mathrm{D}t} &= 2\nu_\mathrm{T}|S|^2 - C_\mu k\omega + \nabla\cdot[(\nu+\sigma_\mathrm{k}(k/\omega))\nabla k],\\ \frac{\mathrm{D}\omega}{\mathrm{D}t} &= 2C_{\omega_1}|S|^2 - C_{\omega_2}\omega^2 + \nabla\cdot[(\nu+\sigma_\omega(k/\omega))\nabla\omega].\end{aligned} \qquad 26.$$

The closure of Equation 25 is

$$-\boldsymbol{\tau} = 2\nu_\mathrm{T}\mathbf{S} - {}^2\!/_3\, k\mathbf{I}, \qquad 27.$$

where $\nu_\mathrm{T} = k/\omega$ and $\mathbf{S}$ is the rate of strain tensor, $S_{ij} = {}^1\!/_2(\partial_j U_i + \partial_i U_j)$. More correctly, this is the RANS formulation; in hybrid simulations some aspect of Equation 26 or Equation 27, or both, is modified to enable eddying.

4.1. Blended Formulations

The nonzonal, but not seamless, approach is to stitch together a RANS and an LES subgrid scale (SGS) model (Fröhlich & Von Terzi 2008). A function of the ratio of grid dimension to turbulence scale $f(\Delta/\Lambda)$ is introduced such that $f(\infty) = 0$ and $f(0) = 1$. The stress models are combined as

$$\boldsymbol{\tau} = (1-f)\boldsymbol{\tau}^\mathrm{RANS} + f\boldsymbol{\tau}^\mathrm{SGS}. \qquad 28.$$

The flow simulation methodology model (Speziale 1998, Fasel et al. 2002) is of this form, with $\boldsymbol{\tau}^\mathrm{SGS} = 0$. It is described as a blend of RANS and DNS. However, hybrid simulation is meant for grids too coarse for DNS, so it could just as well be described as a blend of RANS with implicit LES—which means that numerical diffusion acts as $\boldsymbol{\tau}^\mathrm{SGS}$. An algebraic stress model (see Section 2.2) is adopted by Fasel et al. (2002) for $\boldsymbol{\tau}^\mathrm{RANS}$ along with the $k-\varepsilon$ model. The Kolmogoroff scale $\eta = (\nu^3/\varepsilon)^{1/4}$ is used as the turbulence length scale and the blending function is $f = \exp(-0.004\Delta/\eta)$.

Walters et al. (2013) and Bhushan & Walters (2012) evaluated the interpolation function dynamically by taking the inner product of the rate of strain tensor S_{ij} with Equation 28 and solving

$$1 - f = \frac{\langle\boldsymbol{\tau} - \boldsymbol{\tau}^\mathrm{SGS}\rangle : \langle\mathbf{S}\rangle}{\langle\boldsymbol{\tau}^\mathrm{RANS} - \boldsymbol{\tau}^\mathrm{SGS}\rangle : \langle\mathbf{S}\rangle}. \qquad 29.$$

The stress difference in the numerator is the resolved stress, as calculated during the simulation. This formula is clipped so that f is constrained to lie between 0 and 1. Walters et al. (2013) invoked implicit LES; that is, they relied on numerical diffusion in place of an explicit model for τ^SGS. The eddy viscosity constitutive formula in Equation 27, with the $k-\omega$-SST eddy viscosity, was used for the RANS stress. Bhushan & Walters (2012) invoked the dynamic Smagorinsky, subgrid model for τ^SGS and the S-A RANS model.

Uribe et al. (2010) attributed the idea for their two-velocities model to Schumann (1975). It is of the form of Equation 28 with

$$\begin{aligned} \tau_{ij}^{\mathrm{RANS}} - {}^1\!/_3\,\delta_{ij}\tau_{kk}^{\mathrm{RANS}} &= 2\nu_{\mathrm{T}}\langle S_{ij}\rangle, \\ \tau_{ij}^{\mathrm{SGS}} - {}^1\!/_3\,\delta_{ij}\tau_{kk}^{\mathrm{SGS}} &= 2\nu_{\mathrm{SGS}}(S_{ij} - \langle S_{ij}\rangle), \end{aligned} \qquad 30.$$

where the angle brackets represent an ensemble average: It is computed as a running average over about 10 eddy turnover times. For ν_{T} they use the $\phi - f$ model (Laurence et al. 2004), in which the eddy viscosity is $\nu_{\mathrm{T}} = C_\mu \phi k T$, where T is the turbulence timescale. The subgrid viscosity ν_{SGS} is the Smagorinsky form, $(C_{\mathrm{s}}\Delta)^2|\mathbf{S} - \langle \mathbf{S}\rangle|$. In this case, Λ is the integral scale, $\phi k^{3/2}/\varepsilon$. In this formulation, at any point in the flow domain, two different velocity fields, U and $\langle U \rangle$, coexist. This allows automatic, dynamic switching between RANS and LES as a function of the grid resolution compared to Λ. Xiao & Jenny (2012) took the two-velocity concept a step farther, and computed simultaneous, coupled RANS and LES fields on two different grids.

All these models are validated in channel flow, boundary layers, or more complex geometries, and are shown to be effective. In general, hybrid models improve the prediction of reattachment lengths.

4.2. Seamless Methods

Another class of nonzonal method—which satisfy the present criterion for being seamless—modifies coefficients of a RANS model via a function of the ratio of grid dimension to turbulence scale Δ/Λ. These include the partially integrated transport model (PITM) (Chaouat & Schiestel 2005, 2012) and the partially averaged Navier–Stokes (PANS) model (Girimaji & Abdol-Hamid 2005). In these methods, Λ is the integral scale $k^{3/2}/\varepsilon$. They are framed around the destruction term in the ε equation. This has a coefficient C_{ε_2} equal to 1.92. In PITM, it is replaced with

$$C_{\varepsilon_2}^* = C_{\varepsilon_2} + f(\Delta/\Lambda)(C_{\varepsilon_1} - C_{\varepsilon_2}),$$

where the constant $C_{\varepsilon_1} = 1.44$ is the coefficient of the production term in the ε equation. Thus, when the grid is coarse $C_{\varepsilon_2}^*$ becomes C_{ε_2}; on a fine grid, it becomes C_{ε_1}.

The manner in which this allows eddying is not entirely clear. Chaouat & Schiestel (2005) argued that when the RANS formulation is acting as a subgrid model, it is transferring resolved kinetic energy to subgrid energy and dissipating that energy. When $C_{\varepsilon_2} = C_{\varepsilon_1}$, an equilibrium solution exists in which production equals dissipation. Then the balance between production and dissipation makes the subgrid model directly dissipative, as needed for LES.

Another, more direct explanation, is that reducing $C_{\varepsilon_2}^*$ increases dissipation ε, which in turn reduces k. In combination, these reduce the eddy viscosity $C_\mu k^2/\varepsilon$, enabling the LES mode. PANS operates similarly to PITM, although it modifies both the production and destruction terms in the ε equation to enable a balance where production equals dissipation, and to reduce the eddy viscosity.

Fadai-Ghotbi et al. (2010) invoked the PITM method in conjunction with an elliptic blending Reynolds stress model (see Section 2.1). In PITM and PANS, $f(\Delta/\Lambda)$ originates as a ratio r of modeled to total turbulent kinetic energy, which is developed into a function of Δ/Λ. Fadai-Ghotbi et al. (2010) reverted to the initial idea, basing r on a ratio of the modeled to the actual, computed total kinetic energy. This was done because the PITM formulation for $f(\Delta/\Lambda)$ inhibited eddy formation in channel flow.

These methods have been validated by computer simulation and compared successfully to experimental or DNS data. In some cases the validation is in a very simple geometry, like channel

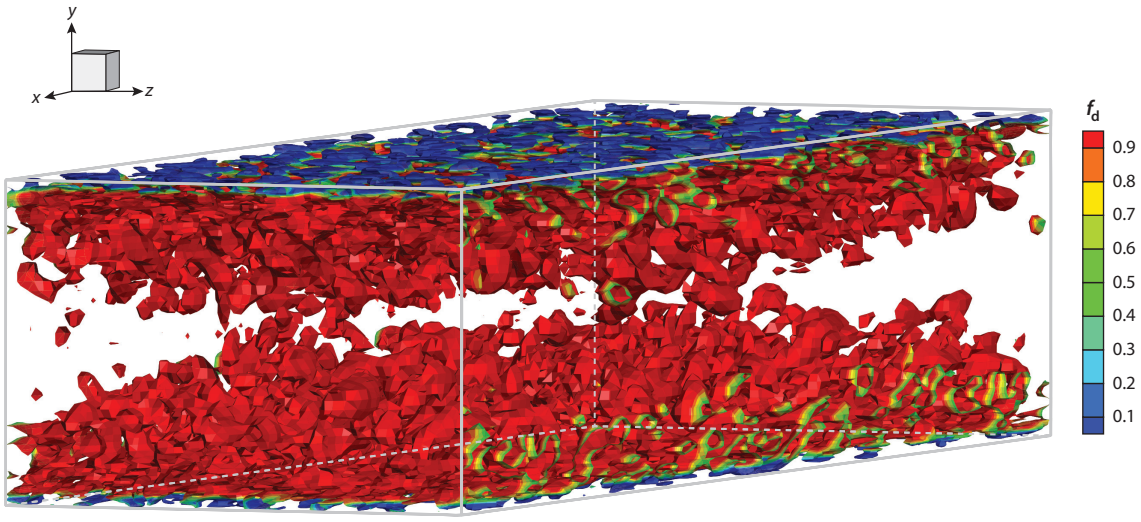

Figure 2

Q contours colored by a shielding function f_d in fully developed channel flow. The region where $f_d \sim 0$ (*blue*) is termed the RANS region. Figure courtesy of Dr. Zifei Yin.

flow or a flat plate boundary layer, and it is unclear how robust the method is. None of these methods has the widespread use enjoyed by the next class of methods.

4.3. Detached-Eddy Simulation

Hybrid RANS/LES models are considered to have promise for industrial CFD applications. The idea is to rely heavily on a closure model in the near-wall part of attached boundary layers and on eddy-resolving simulation in regions away from the surface. The most popular seamless hybrid is detached-eddy simulation (DES) (Spalart 2009). Although DES has some similarity with the methods reviewed above, more than them, it is seen in the vein of enabling a coarser near-wall mesh than would be required for LES.

It appears incongruous for a hybrid to be both an ensemble average (RANS) and a realization (LES). DES is better described as a length scale formulation that adopts either a RANS formula, or a grid dimension, as in LES. It is, everywhere, a realization that has to be averaged to obtain statistics. Significant levels of fluctuations usually are seen, even in parts of the domain that are labeled RANS regions. In delayed DES (DDES), a shielding function f_d is introduced, and $f_d \sim 0$ is called the RANS region, as shown in **Figure 2**.

Figure 3 portrays instantaneous and averaged Q contours on a 10 million–cell RANS mesh. This is a simulation of air flow in a prototype combustor atomizer, computed by adaptive DDES (Ryon 2016). It illustrates that DES resolves turbulent eddies. The averaged field is computed by ensemble averaging the simulation. **Figure 3*c*** shows a purely RANS computation and includes a greater length of the domain than **Figure 3*a*,*b***. The ensemble average is similar to the RANS computation, but at considerably greater computational cost. The cost is warranted if accuracy is improved, or if space-time turbulence structure is needed. Both justifications apply to this atomizer study.

DES originated as the simple formula $\ell = \min[\ell_{RANS}, C_{DES}\Delta]$, where Δ is the grid spacing (Spalart 2000). So the RANS region is that in which the first term is smallest. In most cases, the

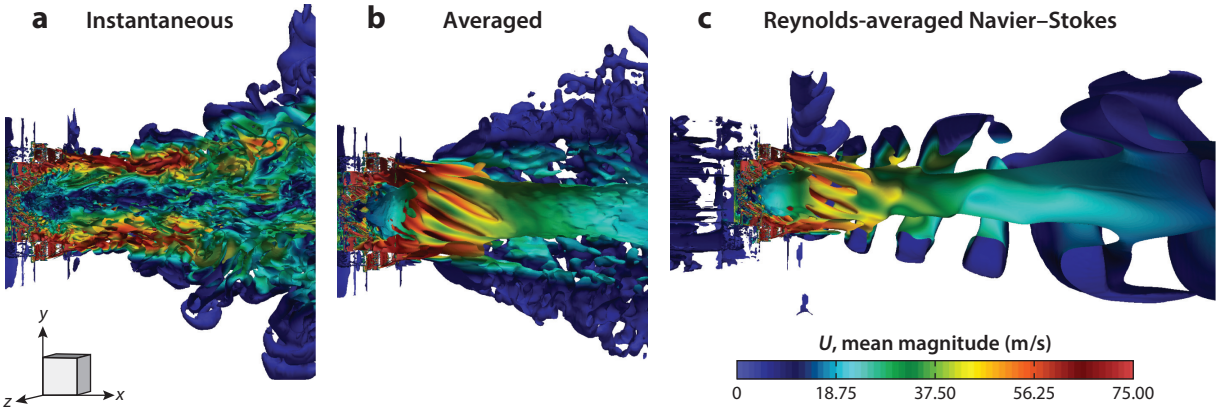

Figure 3

(*a*) Instantaneous and (*b*) ensemble-averaged Q contours colored by U from a detached-eddy simulation of an air blast atomizer. (*c*) A Reynolds-averaged Navier–Stokes (RANS) solution is shown for comparison. Figure adapted with permission from Ryon (2016).

RANS region is next to walls; however, DES is not a wall model per se. Generally, where the grid is coarse compared to the requirements for LES, DES will adopt the RANS length scale; where the grid is fine, it will adopt grid spacing.

Since it was was first proposed, DES has undergone considerable revision, as reviewed by Spalart (2009). An early fault was the occurrence of grid-induced separation, which was attributed to a shortage of resolved stress in intermediate regions where eddy viscosity is decreasing, but resolved stresses have not developed fully. In order to alleviate this, Spalart et al. (2006) introduced the shielding function $f_{\rm d}$. Also, the notion that the method was only for simulating eddying in detached shear layers gave way to a more general view of hybrid, eddy-resolving simulation—so that the D (detached) in DES is not to be taken literally. This more general view initially met a hurdle. Attempts at channel flow simulation (Piomelli et al. 2003) resulted in two mismatched log layers: one from the RANS branch and the other from the LES branch. This anomaly was termed log-layer mismatch and led to other modifications of DDES, such as improved DDES (see Spalart's 2009 review) and vorticity-aligned length scales (Shur et al. 2015).

Originally, DDES was developed for the S-A, eddy viscosity transport model. In that case, the RANS length scale is the wall distance, which enters a dissipation term. The method was applied by Strelets (2001) to the two-equation, $k-\omega$ model. He followed precedent, rewriting the dissipation term $C_\mu k/\omega$ as $C_\mu k^{3/2}/\ell$ in the k-component of Equation 26 in order to phrase it in terms of a dissipation length scale, and then used the DDES length scale formulation of Equation 32. Hanjalić & Kenjereš (2008) described a similar approach due to Hadžiabdić (2005), based on the dissipation term in the $k-\varepsilon$ model. Gritskevich et al. (2012) adopted the Strelets formulation directly. Ashton et al. (2012) developed a variant that used the elliptic relaxation $\phi-f$ model (see Section 2.1). Jee & Shariff (2014) developed a version based on the elliptic relaxation v^2-f model. In addition to the dissipation length scale, they introduced the timescale $\ell_{\rm DES}/\sqrt{k}$, and obtained especially good results for flow over an airfoil.

Reddy et al. (2014) developed a different approach, writing the eddy viscosity as $\nu_{\rm T}=\ell^2\omega$. Correspondingly, the production term in the k-component of Equation 26 becomes $2\nu_{\rm T}|S|^2=2\ell^2\omega|S|^2$. Hence, in this formulation, the lower limit on dissipation in the Strelets (2001) approach

is replaced by an upper limit on production. Again, the DDES length scale (Equation 32) was invoked. Importantly, the switch to the $\ell^2 - \omega$ formulation facilitated the development of adaptive DDES, as described below.

The DDES length-scale model is

$$\begin{aligned} \ell_{\mathrm{DDES}} &= l_{\mathrm{RANS}} - f_{\mathrm{d}}(r_{\mathrm{d}}) \max(0, l_{\mathrm{RANS}} - l_{\mathrm{ES}}), \\ r_{\mathrm{d}} &= \frac{k/\omega + \nu}{\kappa^2 d_{\mathrm{w}}^2 \sqrt{|S|^2 + |\Omega|^2}}, \\ l_{\mathrm{RANS}} &= \sqrt{k}/\omega, \qquad l_{\mathrm{ES}} = C_{\mathrm{DES}} \Delta, \end{aligned} \tag{31.}$$

where Strelets (2001) used $\Delta = h_{\max}$ and Reddy et al. (2014) use $\Delta = V^{1/3}$. V is the cell volume, $h_{\max}$ is the maximum cell dimension, and d_{w} is the wall distance. The shielding function f_{d} ensures a near-wall RANS region on any grid. It has the limits $f_{\mathrm{d}}(\infty) = 0$ and $f_{\mathrm{d}}(0) = 1$.

Yin et al. (2015) and Yin & Durbin (2016) made the $\ell^2 - \omega$ model adaptive by using the dynamic procedure of LES (Lilly 1992),

$$C_{\mathrm{dyn}}^2 = \max[L_{ij} M_{ij} / 2 M_{ij} M_{ji}, 0], \tag{32.}$$

in which the test filter stress and rate of strain,

$$\begin{aligned} L_{ij} &= -\widehat{u_i u_j} + \hat{u}_i \hat{u}_j, \\ M_{ij} &= \hat{\Delta}^2 \hat{\omega} \hat{S}_{ij} - \Delta^2 \widehat{\omega S_{ij}}, \end{aligned} \tag{33.}$$

are computed from the resolved velocity field **u** by local averaging—indicated by the caret. The DES coefficient is given by

$$C_{\mathrm{DES}} = \max(C_{\mathrm{lim}}, C_{\mathrm{dyn}}).$$

The lower bound $C_{\mathrm{lim}}(h_{\max}/\eta)$ prevents spuriously low values of C_{DES} on grids that are too coarse for the dynamic procedure. It compares grid size to an estimated Kolmogoroff scale, $\eta = (\nu^3/\varepsilon_{\mathrm{est}})^{1/4}$, where $\varepsilon_{\mathrm{est}} = k\omega$. As $h_{\max}/\eta \to \infty$, $C_{\mathrm{lim}} \to 0.12$ is the default, coarse grid limit. When $h_{\max}/\eta \ll 20$, $C_{\mathrm{lim}} \sim 0$, so C_{DES} is constrained only to be nonnegative.

An indirect effect of the dynamic, local evaluation of C_{DES} is that the shielded region shrinks when the grid is relatively fine (**Figure 4*a***). $f_{\mathrm{d}} \sim 1$ is the turbulence-resolving region. The f_{d} curve starts to rise when y_+ is less than 10; the turbulence already is resolved in the log layer where $y_+ > 40$. The rational limit, that DES → wall-resolved LES as the grid is refined, can be accomplished by adaptive DES (Yin & Durbin 2016).

The adaptive model reverts to nonadaptive behavior on coarse grids (**Figure 4*c*,*d***). The nonzonal character of DES is also illustrated by the f_{d} curves: The RANS region is not of a fixed thickness, varying from one case to the next.

Data-driven: term used to describe models that extract information from data, without regard to phenomenology

5. DATA-DRIVEN MODELING

Large sets of Reynolds-averaged data have been created by DNS and advanced measurement methods. It has long been speculated that these might lead to improvements of turbulence models. However, the large data sets have mostly been used in the same manner as older, more limited data sets: that is, they are plotted along with model predictions to assess model accuracy by comparison. Certainly, channel flow DNS data have been especially useful for compute-and-compare assessment and development of models. However, there is a persistent sense that data-driven methods have had too little impact on closure modeling.

Parneix et al. (1998) proposed that DNS data might be used more comprehensively to assess models. Some terms in the governing equations can be taken from data, and the model's ability to

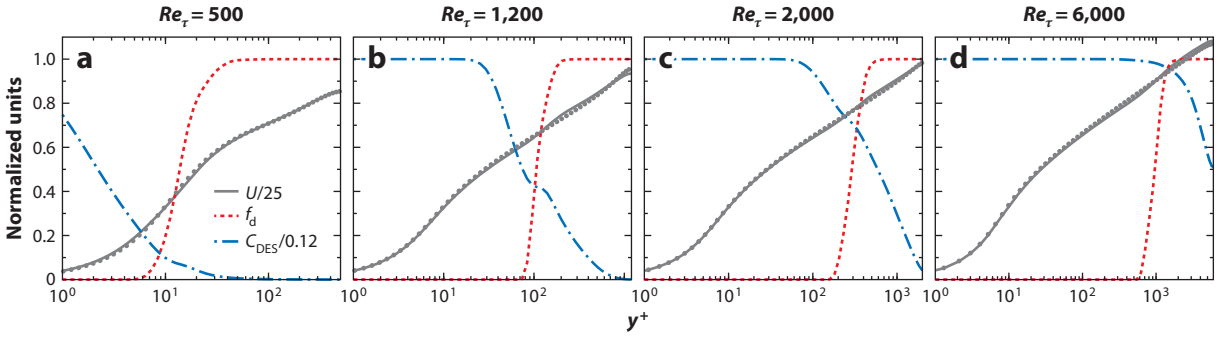

Figure 4

Adaptive detached-eddy simulation (DES) solution in plane channel flow. The grid spacing is fixed and $\Delta x^+ = 0.1 Re_\tau$. Figure adapted with permission from Yin et al. (2015).

predict others can be assessed. For instance, $\varepsilon(\mathbf{x})$ can be taken from a DNS field of data, removing the suspicious ε equation from the model. Actually, Parneix et al. (1998) concluded that the ε equation was not the cause of poor predictions in flow over a backward-facing step. Raiesi et al. (2011) applied a similar method to LES data sets. As one example, they used a field of k from LES data and solved the ω equation of the $k-\omega$ model. Not surprisingly, using accurate k deteriorates the accuracy of the $k-\omega$ model (one could say that the k of the $k-\omega$ model should not be interpreted as the turbulent kinetic energy). Raiesi et al. (2011) also took k and ε from LES and solved the ζ and ϕ equations of the $\zeta-\phi$ model. Ling et al. (2013) used experimentally measured velocity and thermal fields and obtained an eddy diffusivity by optimizing the fit between model and data. Regrettably, these studies have not led to insights into improving closure models.

Recently, an approach termed inverse modeling was advocated by Dow & Wang (2010, 2011), Duraisamy et al. (2015), and Parish & Duraisamy (2016). It has been applied to transition (Duraisamy & Durbin 2014) and turbulence models. Dow & Wang (2010) provided a simple exposition of the method for plane channel flow.

Inverse modeling evolved out of adjoint-based, optimization methods for aerodynamic design. A fundamental juggernaut to using data more comprehensively has been the ambiguous connection between model variables—$\omega(\mathbf{x})$, $\nu_\Gamma(\mathbf{x})$, $\gamma(\mathbf{x})$, etc.—and physically measurable quantities. Model variables are an invention of the closure scheme. Inverse modeling treats them as parameters to be found by minimizing a cost function. For instance, the cost function may be the weighted mean-squared error

$$E = \sum_i |Q^i - Q^i_{\text{data}}|^2 w_i \qquad 34.$$

of a predicted variable Q, relative to an array of data Q_{data}. If a model variable $\phi(\mathbf{x})$ is to be found, it is treated as a parameter field and

$$\min_{\phi(x_n)} E$$

is solved, where n includes all grid points. In the approach proposed by Duraisamy et al. (2015), instead of directly finding the turbulence variable, a corrective coefficient α is inserted into its governing equation. One writes

$$\frac{\mathrm{D}\phi}{\mathrm{D}t} = \alpha(\mathbf{x}) \times \text{Source} - \text{Sink} + \text{Diffusion} \qquad 35.$$

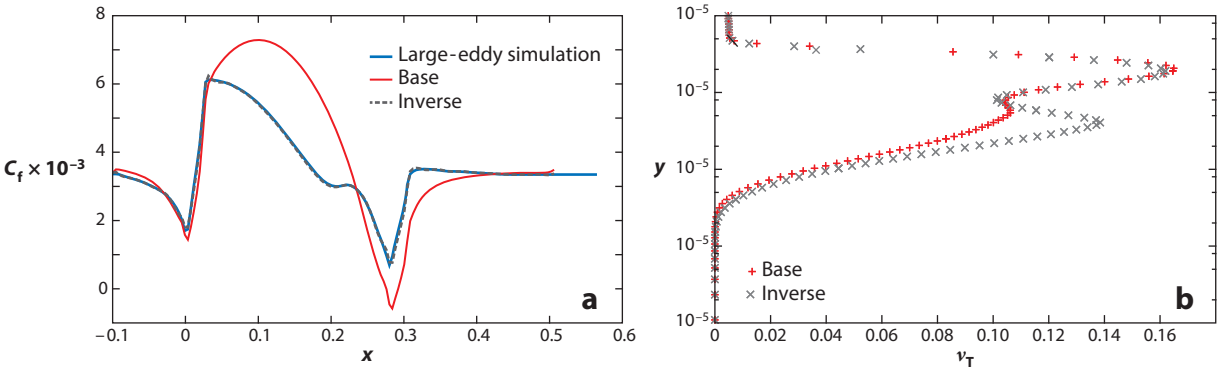

Figure 5

Data extraction by optimization. (*a*) The base solution and an optimized fit to LES data for C_f in flow over a slender bump. (*b*) An extracted eddy viscosity profile along with a solution to the base model. Figure courtesy of Racheet Matai.

and $\min_{\alpha(x_n)} E$ is solved, starting from the initial guess $\alpha \equiv 1$. Thereby, one obtains a field of the variable of interest, e.g., $\omega(\mathbf{x})$. Hence, data on $\omega(\mathbf{x})$ are extracted from data on the flow field by solving the ω equation with the optimal correction α. The method is illustrated by **Figure 5**, in which an optimized fit to skin friction data is used to extract an eddy viscosity profile.

Inverse modeling is attractive because data for model variables are extracted by using those variables in their intended context. In a RANS computation, predictions of quantities like skin friction or the velocity field are global consequences of model variables. Therefore, as the cost function is minimized, at each iteration, the full RANS equations must be solved.

In the adjoint method, the gradient of the cost function is found by solving linear, adjoint equations (Giles & Pierce 2000). The adjoint solution functions as sensitivity coefficients that weight regions where the corrective function has its largest impact on the discrepancy between prediction and input data.

To date, this has been a method to extract data on model variables. It has yet to lead to improved prediction methods. Extracted data are functions of position in a given geometry $\alpha(x)$. Research is in progress to convert this into model improvements by correlating α with coordinate independent parameters, using methods of machine learning such as neural nets or kernel regression (Tracey et al. 2013, Parish & Duraisamy 2016).

6. OUTLOOK

Over the years, the notion that closure modeling will be replaced by eddy-resolved simulation has been advanced and abandoned (Laurence 2002, Hanjalić 2005, Hanjalić & Kenjereš 2008, Spalart 2010, Slotnick et al. 2014). Mark Twain is often reported to have quipped, "reports of my death have been greatly exaggerated." It is a matter of extrapolation, not prophecy, that RANS closure models will remain an essential element of applied CFD into the foreseeable future. Their marriage with eddy-resolving simulation, under the heading of hybrid methods, adds to their vitality. Hybrid simulation is expanding into new niches where it provides either improved accuracy or space and time fluctuations that are not available from pure RANS solutions for ensemble-averaged fields. At the same time, niches for pure RANS analysis are also expanding as industry and researchers find new applications. Advances in modeling have not kept pace with this burgeoning use.

The basic limitations—that moment equations are unclosed and that closure is accomplished by empiricism—are inescapable: Averaging destroys information and prohibits mathematical rigor. However, this opens the door to pragmatic creativity. Given the widespread use of RANS closure for engineering analysis and for design in a wide range of industries, and given its central role in commercial CFD codes, closure modeling will remain a very attractive area of research.

Many experiments and high-fidelity computer simulations have a stated objective of providing data for modeling. However, large data sets have led to few advances in the way that data are used: Model constants are tuned by eyeballing the fit to data, models are assessed by compute and compare, and discrepancies are noted but not explained any better with big data sets than was done with small ones. There is a need for innovative research into data-driven modeling.

New directions in closure modeling per se will likely be toward expanding the phenomena they incorporate, as illustrated by the ideas reviewed herein for incorporating transition and streamline curvature. Inaccuracies near separation lines and inaccurate reattachment lengths, etc., are long-standing motives for new research. Transition models are evolving and should be improved. There are other phenomena (e.g., effects of surface roughness, wall proximity, shock–turbulence interactions, applications to multiphase flow or plasma dynamics) that support either improving the empiricism or examining new formulations.

Hybrid methods invite further questions: Where is LES more reliable than RANS, and where is it less so? Do various blending, shielding, and interpolation functions plausibly select the most suitable mode? On coarse grids, LES can be grid dependent and hence user dependent; from an industrial perspective, robustness is another concern. Can hybrid methods be made resistant to vagaries of gridding? More accurate Reynolds stress closure models can lead to improvements in hybrid simulation. Should the underlying closures be devised specifically for hybrid modeling? These and other issues deserve attention.

FUTURE ISSUES

1. Improving predictive accuracy remains a driving force in closure modeling. In many industrial applications, accuracy of turbulence models remains the pacing item in CFD analysis.
2. Schemes to incorporate new phenomena into closure models need to be developed. The demand is growing with the breadth of applications.
3. Various routes of laminar to turbulent transition need to be modeled. The challenge is to predict the location of the transition. Precursors may be Tollmien–Schlichting waves, Klebanoff modes, cross-flow instability, Mack modes at high Mach number, streaks caused by surface roughness, stratified and buoyant instability, etc.
4. Hybrid blending functions should select which of RANS or LES is more reliable within regions of a given flow, with a given grid, with a given numerical scheme, and with a given closure model. Is the ratio of grid size to turbulent scale the right metric? Adaptive methods should continue to be developed.
5. Can methods of data-driven science and engineering lead to improved closure models? Comprehensive data fields can be used to test modeled terms or to extract information on turbulence variables. Methods of machine learning are being explored for correlating model term corrections with invariant parameters.

DISCLOSURE STATEMENT

The author is not aware of any biases that might be perceived as affecting the objectivity of this review.

ACKNOWLEDGMENTS

The author's work in the areas of this review has been funded in part by NASA, the National Science Foundation, the Office of Naval Research, the Air Force Office of Scientific Research, and Pratt & Whitney. Suggestions from Prof. Dominique Laurence and Dr. Gorazd Medic are gratefully acknowledged.

LITERATURE CITED

Abu-Ghannam BJ, Shaw R. 1980. Natural transition of boundary layers—the effects of turbulence, pressure gradient, and flow history. *J. Mech. Eng. Sci.* 22:213–28

Arolla SK, Durbin PA. 2013. Modeling rotation and curvature effects within scalar eddy viscosity model framework. *Int. J. Heat Fluid Flow* 39:78–89

Ashton N, Revell A, Prosser R, Uribe J. 2012. Development of an alternative delayed detached-eddy simulation formulation based on elliptic relaxation. *AIAA J.* 51:513–19

Bhushan S, Walters DK. 2012. A dynamic hybrid Reynolds-averaged Navier Stokes–large eddy simulation modeling framework. *Phys. Fluids* 24:015103

Billard F, Laurence D. 2012. A robust $k-\varepsilon-\overline{v^2}/k$ elliptic blending turbulence model applied to near-wall, separated and buoyant flows. *Int. J. Heat Fluid Flow* 33:45–58

Billard F, Revell A, Craft T. 2012. Application of recently developed elliptic blending based models to separated flows. *Int. J. Heat Fluid Flow* 35:141–51

Bose S, Park GI. 2018. Wall-modeled LES for complex turbulent flows. *Annu. Rev. Fluid Mech.* 50:535–61

Canuto VM, Howard A, Cheng Y, Dubovikov MS. 2001. Ocean turbulence. Part I: one-point closure model—momentum and heat vertical diffusivities. *J. Phys. Oceanogr.* 31:1413–26

Chaouat B, Schiestel R. 2005. A new partially integrated transport model for subgrid-scale stresses and dissipation rate for turbulent developing flows. *Phys. Fluids* 17:065106

Chaouat B, Schiestel R. 2012. Analytical insights into the partially integrated transport modeling method for hybrid Reynolds averaged Navier-Stokes equations-large eddy simulations of turbulent flows. *Phys. Fluids* 24:085106

Choi SK, Kim SO. 2006. Computation of a turbulent natural convection in a rectangular cavity with the elliptic-blending second-moment closure. *Int. Commun. Heat Mass Transf.* 33:1217–24

Choi SK, Kim SO. 2008. Treatment of turbulent heat fluxes with the elliptic-blending second-moment closure for turbulent natural convection flows. *Int. Commun. Heat Mass Transf.* 51:2377–88

Dassler P, Kožulović D, Fiala A. 2010. Modelling of roughness-induced transition using local variables. *Proc. ECCOMAS Eur. Conf. Comput. Fluid Dyn., 5th*, ed. JCF Pereira, A Sequeira, JMC Pereira, Pap. 01811

Dehoux F, Benhamadouche S, Manceau R. 2017. An elliptic blending differential flux model for natural, mixed and forced convection. *Int. J. Heat Fluid Flow.* 63:190–204

Dehoux F, Lecocq Y, Benhamadouche S, Manceau R, Brizzi LE. 2011. Algebraic modeling of the turbulent heat fluxes using the elliptic blending approach—application to forced and mixed convection regimes. *Flow Turbul. Combust.* 88:77–100

Dhawan S, Narasimha R. 1958. Some properties of boundary layer during the transition from laminar to turbulent flow motion. *J. Fluid Mech.* 3:418–36

Dow E, Wang Q. 2010. Quantification of structural uncertainties in the $k-\omega$ turbulence model. *Proc. Summer Program 2010*, pp. 41–51. Stanford, CA: Cent. Turb. Res.

Dow E, Wang Q. 2011. *Uncertainty quantification of structural uncertainties in RANS simulations of complex flows*. Presented at AIAA Comput. Fluid Dyn. Conf., 20th, June 27–30, Honolulu, HI, AIAA Pap. 2011-3865

Duraisamy K, Durbin PA. 2014. Transition modeling using data driven approaches. *Proc. Summer Program 2014*, pp. 427–34. Stanford, CA: Cent. Turb. Res.

Duraisamy K, Zhang Z, Singh AP. 2015. *New approaches in turbulence and transition modeling using data-driven techniques*. Presented at AIAA Aerosp. Sci. Meet., 53rd, Jan. 5–9, Kissimmee, FL, AIAA Pap. 2015-1284

Durbin PA. 1993. A Reynolds stress model for near-wall turbulence. *J. Fluid Mech.* 249:465–98

Durbin PA. 2011. Review: adapting scalar turbulence closure models for rotation and curvature. *J. Fluids Eng.* 133:061205

Durbin PA. 2012. An intermittency model for bypass transition. *Int. J. Heat Fluid Flow* 36:1–6

Durbin PA, Pettersson-Reif BA. 2010. *Statistical Theory and Modeling for Turbulent Flow*. New York: Wiley. 2nd ed.

Fadai-Ghotbi A, Friess C, Manceau R, Borée J. 2010. A seamless hybrid RANS-LES model based on transport equations for the subgrid stresses and elliptic blending. *Phys. Fluids* 22:055104

Fasel HF, Seidel J, Wernz S. 2002. A methodology for simulations of complex turbulent flows. *J. Fluids Eng.* 124:933–42

Franke M, Wallin S, Thiele F. 2005. Assessment of explicit algebraic Reynolds-stress turbulence models in aerodynamic computations. *Aerosp. Sci. Technol.* 9:573–81

Fröhlich J, Von Terzi D. 2008. Hybrid LES/RANS methods for the simulation of turbulent flows. *Prog. Aerosp. Sci.* 44:349–77

Gatski TB, Jongen T. 2000. Nonlinear eddy viscosity and algebraic stress models for solving complex turbulent flows. *Prog. Aerosp. Sci.* 36:655–82

Gatski TB, Rumsey CL. 2002. Linear and nonlinear eddy viscosity models. In *Closure Strategies for Turbulent and Transitional Flows*, ed. B Launder, N Sandham, pp. 9–46. Cambridge, UK: Cambridge Univ. Press

Gatski TB, Speziale CG. 1993. On explicit algebraic stress models for complex turbulent flows. *J. Fluid Mech.* 254:59–78

Ge X, Arolla S, Durbin PA. 2014. A bypass transition model based on the intermittency function. *Flow Turbul. Combust.* 93:37–61

Ge X, Durbin PA. 2015. An intermittency model for predicting roughness induced transition. *Int. J. Heat Fluid Flow* 54:55–64

Giles MB, Pierce NA. 2000. An introduction to the adjoint approach to design. *Flow Turbul. Combust.* 65:393–415

Girimaji S, Abdol-Hamid K. 2005. *Partially-averaged Navier Stokes model for turbulence: implementation and validation*. Presented at AIAA Aerosp. Sci. Meet., 43rd, Jan. 10–13, Reno, NV, AIAA Pap. 2005-502

Gritskevich MS, Garbaruk AV, Schultze J, Menter FR. 2012. Development of DDES and IDDES formulations for the $k-\omega$ shear stress transport model. *Flow Turbul. Combust.* 88:431–49

Hadžiabdić M. 2005. *LES, RANS and combined simulation of impinging flows and heat transfer*. PhD Thesis, Delft Univ. Technol.

Hanjalić K. 2005. Will RANS survive LES? A view of perspectives. *J. Fluids Eng.* 127:831–39

Hanjalić K, Kenjereš S. 2008. Some developments in turbulence modeling for wind and environmental engineering. *J. Wind Eng. Ind. Aerodyn.* 96:1537–70

Hanjalić K, Launder BE. 2011. *Modelling Turbulence in Engineering and the Environment: Second-Moment Routes to Closure*. Cambridge, UK: Cambridge Univ. Press

Hanjalić K, Popovac M, Hadziabdic M. 2004. A robust near-wall elliptic relaxation eddy-viscosity turbulence model for CFD. *Int. J. Heat Fluid Flow* 25:1047–51

Hellsten A. 1998. *Some improvements in Menter's $k-\omega$ SST turbulence model*. Presented at AIAA Fluid Dyn. Conf., 29th, June 15–18, Albuquerque, NM, AIAA Pap. 98-2554

Hodson HP, Howell RJ. 2005. Bladerow interactions, transition, and high-lift aerofoils in low-pressure turbines. *Annu. Rev. Fluid Mech.* 37:71–98

Jee S, Shariff K. 2014. Detached-eddy simulation based on the v^2-f model. *Int. J. Heat Fluid Flow* 46:84–101

Ji M, Durbin PA. 2004. On the equilibrium states predicted by second moment models in rotating, stably stratified homogeneous shear flow. *Phys. Fluids* 16:3540–56

Kenjereš S, Gunarjo S, Hanjalić K. 2005. Contribution to elliptic relaxation modelling of turbulent natural and mixed convection. *Int. J. Heat Fluid Flow* 26:569–86

Khodak A, Hirsch C. 1996. Second order non-linear $k-\varepsilon$ models with explicit effect of curvature and rotation. *Proc. ECCOMAS Eur. Conf. Comput. Fluid Dyn., 3rd, 1996*, ed. J-A Désidéri, pp. 690–96. Chichester, NY: Wiley

Kubacki S, Dick E. 2016. An algebraic model for bypass transition in turbomachinery boundary layer flows. *Int. J. Heat Fluid Flow* 58:68–83

Langtry RB, Menter FR. 2005. *Transition modeling for general CFD applications in aeronautics*. Presented at AIAA Aerosp. Sci. Meet., 43rd, Jan. 10–13, Reno, NV, AIAA Pap. 2005-522

Lardeau S, Billard F. 2016. *Development of an elliptic-blending lag model for industrial applications*. Presented at AIAA Aerosp. Sci. Meet., 54th, Jan. 4–8, San Diego, CA, AIAA Pap. 2016-1600

Lardeau S, Leschziner M, Li N. 2004. Modelling bypass transition with low-Reynolds-number nonlinear eddy-viscosity closure. *Flow Turbul. Combust.* 73:49–76

Launder BE. 1989. Second-moment closure: present...and future? *Int. J. Heat Fluid Flow* 10:282–300

Laurence D. 2002. Large eddy simulation of industrial flows? In *Closure Strategies for Turbulent and Transitional Flows*, ed. BE Launder, ND Sandham, pp. 392–406. Cambridge, UK: Cambridge Univ. Press

Laurence D, Uribe J, Utyuzhnikov S. 2004. A robust formulation of the v^2-f model. *Flow Turbul. Combust.* 73:169–85

Leschziner M. 2016. *Statistical Turbulence Modelling for Fluid Dynamics—Demystified: An Introductory Text for Graduate Engineering Students*. London: Imperial Coll. Press

Lilly DK. 1992. A proposed modification of the Germano subgrid-scale closure method. *Phys. Fluids A* 4:633–45

Ling J, Coletti F, Yapa SD, Eaton JK. 2013. Experimentally informed optimization of turbulent diffusivity for a discrete hole film cooling geometry. *Int. J. Heat Fluid Flow* 44:348–57

Liu Y, Zaki TA, Durbin PA. 2008. Boundary layer transition by interaction of discrete and continuous modes. *J. Fluid Mech.* 604:199–233

Lodefier K, Merci B, De Langhe C, Dick E. 2004. Transition modelling with the $k-\omega$ turbulence model and an intermittency transport equation. *J. Therm. Sci.* 13:220–25

Lopez M, Walters DK. 2016. Prediction of transitional and fully turbulent flow using an alternative to the laminar kinetic energy approach. *J. Turbul.* 17:253–73

Manceau R. 2005. An improved version of the elliptic blending model. Application to non-rotating and rotating channel flows. *Proc. Int. Symp. Turbul. Shear Flow Phenom., 4th*, pp. 259–64. **http://www.tsfp-conference.org/proceedings/2005/tsfp4-ca-2.pdf**

Manceau R. 2015. Recent progress in the development of the elliptic blending Reynolds-stress model. *Int. J. Heat Fluid Flow* 51:195–220

Manceau R, Hanjalić K. 2002. Elliptic blending model: a new near-wall Reynolds-stress turbulence closure. *Phys. Fluids* 14:744–54

Manceau R, Wang M, Laurence D. 2001. Inhomogeneity and anisotropy effects on the redistribution term in Reynolds-averaged Navier-Stokes modelling. *J. Fluid Mech.* 438:307–38

Mayle RE. 1991. The 1991 IGTI scholar lecture: the role of laminar-turbulent transition in gas turbine engines. *J. Turbomach.* 113:509–36

Medida S, Baeder J. 2011. Numerical prediction of static and dynamic stall phenomena using the $\gamma-R_\theta$ transition model. *Am. Helicopter Soc. Annu. Forum, 67th*, 3–5 *May*, *Virgina Beach*, *Va.*, pp. 431–54. Redhook, NY: Curran. **http://toc.proceedings.com/11701webtoc.pdf**

Mellor GL, Yamada T. 1982. Development of a turbulence closure model for geophysical fluid problems. *Rev. Geophys. Space Phys.* 20:851–75

Menter FR, Langtry RB, Völker S. 2006. Transition modeling for general purpose CFD codes. *Flow Turbul. Combust.* 77:277–303

Menter FR, Smirnov PE, Liu T, Avancha R. 2015. A one-equation local correlation-based transition model. *Flow Turbul. Combust.* 95:583–619

Parish EJ, Duraisamy K. 2016. A paradigm for data-driven predictive modeling using field inversion and machine learning. *J. Comput. Phys.* 305:758–74

Parneix S, Laurence D, Durbin PA. 1998. A procedure for using DNS databases. *J. Fluids Eng.* 120:40–47

Pecnik R, Pieringer P, Sanz W. 2005. Numerical investigation of the secondary flow of a transonic turbine stage using various turbulence closures. *ASME Turbo Expo 2005: Power Land Sea Air, June 6–9, Reno, NV*, Vol. 6, pp. 1185–93. New York: Am. Soc. Mech. Eng.

Piomelli U, Balaras E, Pasinato H, Squires KD, Spalart PR. 2003. The inner-outer layer interface in large-eddy simulations with wall-layer models. *Int. J. Heat Fluid Flow* 24:538–50

Pope SB. 1975. A more general effective-viscosity hypothesis. *J. Fluid Mech.* 72:331–40

Pope SB. 2001. *Turbulent Flows*. Cambridge, UK: Cambridge Univ. Press

Raiesi H, Piomelli U, Pollard A. 2011. Evaluation of turbulence models using direct numerical and large-eddy simulation data. *J. Fluids Eng.* 133:021203

Reddy KR, Ryon JA, Durbin PA. 2014. A DDES model with a Smagorinsky-type eddy viscosity formulation and log-layer mismatch correction. *Int. J. Heat Fluid Flow* 50:103–13

Rodi W. 1976. A new algebraic relation for calculating the Reynolds stresses. *Z. Angew. Math. Mech.* 56:T219–21

Rumsey CL, Gatski TB, Morrison JH. 2000. Turbulence model predictions of strongly curved flow in a U-duct. *AIAA J.* 38:1394–402

Ryon J. 2016. *Analysis and design of lean direct injection fuel nozzles by eddy resolved turbulence simulation*. PhD Thesis, Iowa State Univ.

Savill AM. 1999. One point closures applied to transition. In *Turbulence and Transition*, ed. M Hallbäck, DS Henningson, AV Johansson, PH Alfredson, pp. 233–68. Dordrecht, Neth.: Kluwer Acad.

Schumann U. 1975. Subgrid scale model for finite difference simulations of turbulent flows in plane channels and annuli. *J. Comput. Phys.* 18:376–404

Shin JK, An JS, Choi YD, Kim YC, Kim MS. 2008. Elliptic relaxation second moment closure for the turbulent heat fluxes. *J. Turbul.* 9:N3

Shur ML, Spalart PR, Strelets MK, Travin AK. 2015. An enhanced version of DES with rapid transition from RANS to LES in separated flows. *Flow Turbul. Combust.* 95:709–37

Shur ML, Strelets MK, Travin AK, Spalart PR. 2000. Turbulence modeling in rotating and curved channels: assessing the Spalart-Shur correction. *AIAA J.* 38:784–92

Slotnick J, Khodadoust A, Alonso J, Darmofal D, Gropp W, et al. 2014. *CFD Vision 2030 study: a path to revolutionary computational aerosciences*. NASA Tech. Rep. CR-2014-218178, Langley Res. Cent., Hampton, VA

Spalart PR. 2000. Strategies for turbulence modelling and simulations. *Int. J. Heat Fluid Flow* 21:252–63

Spalart PR. 2009. Detached eddy simulation. *Annu. Rev. Fluid Mech.* 41:181–202

Spalart PR. 2010. Reflections on RANS modelling. In *Progress in Hybrid RANS-LES Modelling: Papers Contributed to the 3rd Symposium on Hybrid RANS-LES Methods, Gdansk, Poland, June 2009*, ed. SH Peng, P Doerffer, W Haase, pp. 7–24. Berlin: Springer-Verlag

Spalart PR, Deck S, Shur ML, Squires KD, Strelets MK, Travin AK. 2006. A new version of detached-eddy simulation, resistant to ambiguous grid densities. *Theor. Comput. Fluid Dyn.* 20:181–95

Spalart PR, Shur ML. 1997. On the sensitization of turbulence models to rotation and curvature. *Aerosp. Sci. Technol.* 1:297–302

Speziale CG. 1991. Analytic methods for the development of Reynolds stress closures in turbulence. *Annu. Rev. Fluid Mech.* 23:107–57

Speziale CG. 1998. Turbulence modeling for time-dependent RANS and VLES: a review. *AIAA J.* 36:173–84

Speziale CG, Sarkar S, Gatski TB. 1991. Modelling the pressure–strain correlation of turbulence: an invariant dynamical systems approach. *J. Fluid Mech.* 227:245–72

Strelets M. 2001. *Detached eddy simulation of massively separated flows*. Presented at AIAA Aerosp. Sci. Meet., 39th, Jan. 8–11, Reno, NV, AIAA Pap. 2001-0879

Suga K, Abe K. 2000. Nonlinear eddy viscosity modelling for turbulence and heat transfer near wall and shear-free boundaries. *Int. J. Heat Fluid Flow* 21:37–48

Suluksna K, Dechaumphai P, Juntasaro E. 2009. Correlations for modeling transitional boundary layers under influences of free stream turbulence and pressure gradient. *Int. J. Heat Fluid Flow* 30:66–72

Suzen YB, Huang PG. 1999. Modeling of flow transition using an intermittency transport equation. *J. Fluids Eng.* 122:273–84

Taulbee DB. 1992. An improved algebraic Reynolds stress model and corresponding nonlinear stress model. *Phys. Fluids A* 4:2555–61

Tracey B, Duraisamy K, Alonso JJ. 2013. *Application of supervised learning to quantify uncertainties in turbulence and combustion modeling*. Presented at AIAA Aerosp. Sci. Meet., 51st, Jan. 7–10, Grapevine, TX, AIAA Pap. 2013-0259

Uribe JC, Jarrin N, Prosser R, Laurence D. 2010. Development of a two-velocities hybrid RANS-LES model and its application to a trailing edge flow. *Flow Turbul. Combust.* 85:181–97

Wallin S, Johansson AV. 2000. An explicit algebraic Reynolds stress model for incompressible and compressible turbulent flows. *J. Fluid Mech.* 403:89–132

Wallin S, Johansson AV. 2002. Modelling streamline curvature effects in explicit algebraic Reynolds stress turbulence models. *Int. J. Heat Fluid Flow* 23:721–30

Walters DK, Bhushan S, Alam MF, Thompson DS. 2013. Investigation of a dynamic hybrid RANS/LES modelling methodology for finite-volume CFD simulations. *Flow Turbul. Combust.* 91:643–67

Walters DK, Cokljat D. 2008. A three-equation eddy-viscosity model for Reynolds-averaged Navier–Stokes simulations of transitional flow. *J. Fluids Eng.* 130:121401

Walters DK, Leylek JH. 2004. A new model for boundary layer transition using a single-point RANS approach. *J. Turbomach.* 126:193–202

Wang L, Fu S. 2011. Development of an intermittency equation for the modeling of the supersonic/hypersonic boundary layer flow transition. *Flow Turbul. Combust.* 87:165–87

Weinmann M, Sandberg R. 2009. *Suitability of explicit algebraic stress models for predicting complex three-dimensional flows*. Presented at AIAA Comput. Fluid Dyn. Conf., 19th, June 22–25, San Antonio, TX, AIAA Pap. 2009-3663

Westin KJA, Henkes RAWM. 1997. Application of turbulence models to bypass transition. *J. Fluids Eng.* 119:859–66

Wilcox DC. 1994. Simulation of transition with a two-equation turbulence model. *AIAA J.* 32:247–55

Wilcox DC. 1998. *Turbulence Modeling for CFD*. Lake Arrowhead, CA: DCW Ind. 2nd ed.

Wu X, Durbin PA. 2000. Boundary layer transition induced by periodic wakes. *J. Turbomach.* 122:442–49

Xiao H, Jenny P. 2012. A consistent dual-mesh framework for hybrid LES/RANS modeling. *J. Comput. Phys.* 231:1848–65

Yin Z, Durbin PA. 2016. An adaptive DES model that allows wall-resolved eddy simulation. *Int. J. Heat Fluid Flow* 62:499–509

Yin Z, Reddy KR, Durbin PA. 2015. On the dynamic computation of the model constant in delayed detached eddy simulation. *Phys. Fluids* 27:025105

Zaki TA. 2013. From streaks to spots and on to turbulence: exploring the dynamics of boundary layer transition. *Flow Turbul. Combust.* 91:451–73

Annual Review of Fluid Mechanics

Volume 50, 2018

Contents

Indexes

Errata

An online log of corrections to *Annual Review of Fluid Mechanics* articles may be found at http://www.annualreviews.org/errata/fluid